

Numerical Studies on Residual Stress and Strain Distribution in Thick-welded Plate

Chand R. R., Kim I. S., Lee J. H., Jung S. M. and Lee J. P.

Department of Mechanical Engineering, Mokpo National University, 61, Dorim-ri, Chungkye-myun, Muan-gun, Jeonnam 534-729, South Korea

Abstract

In this study, a numerical method is used to investigate the effect of welding parameter and cooling time on residual stress and strain in the multi-pass butt Gas Metal Arc (GMA) welding process, while plate is restrained in transverse direction of welding direction. Two dimension finite element simulations were implemented to predict the welding temperature distributions, residual stress and strain on 16mm thick SM490 steel plate for different input welding parameter at each weld pass using Ansys software. Not only the temperature dependent thermal properties were considered, but also birth and death technique is employed to control the process of weld filling. The simulated results provide good evidence that residual stress and strain is mainly dependent on heat load, welding parameter and restraints on material. The large amount of residual stress and strain is being developed around the Heat Affected Zone, Fusion zone and welding regions. The elastic FE model can be used to predict precisely the welding deformation and residual stress in a thick multi pass butt welding. Furthermore, the extensive experiment effort of component testing could be reduced adequate and deliberate application of welding FE simulation.

Keywords: Finite Element Simulations, Fusion Zone, Heat Affected Zone, welding parameter, Residual stress and Strain.

1 Introduction

Gas Metal Arc (GMA) welding process has widely been employed due to the wide range of applications, cheap consumables and easy handling. In order to achieve a high level of welding performance and quality, a suitable model is required to investigate the characteristics for the effects of process parameters on the bead geometry in the GMA welding process. The high local non-uniform heating and subsequent rapid cooling, which takes place during any welding process affects welding parameters such as residual stresses, deformations, weld microstructures and HAZ hardness. The high stress region near the welded zone causes a premature failure of structures because the thermal cycle of multi-pass welding process in butt weld joints are quite complex.

Therefore, development of the numerical model to predict the residual stress and strain is an important task [2-6]. There has been lot of experiment and Finite Element Analysis (FEA) being conducted for predicting the temperature history, residual stress and welding distortion for root pass, and a lot of fundamental knowledge have also been established [1-10]. However, there is very little literature

describing the prediction of temperature history, residual stress and strain distribution on multi-pass butt weld joint. For instance, Heinze developed and simulated FE model, to predict the welding temperature, residual stress and welding distortion fields in multi-pass butt weld joint plate under different welding condition. The author investigated six bead multi-pass gas metal arc weld of 20mm thick structural steel S355J2+N under shrinkage restraints and fundamental prediction has been established [1]. Attarha conducted the study on welding temperature distributions in thin welded plates through experimental measurements and finite element simulation [2].

In other researchers tried to investigate the effect of each temperature-dependent material property on the transient temperatures, residual stresses and distortions in the computational simulation of welding process [3-10]. The mechanical interaction between welded plate and restraint area has much influence on the distribution of residual stress and distortion. Many researchers applied the different rules to the model, trying to predict and reduce the

stress and strain problem in welding process. Still some researchers improved in numerically prediction of welding process and it correlates with the actual welding process. The influencing factors such as welding parameter, peak temperature of thermal cycle and restraint has significant effect on the Fusion zone (FZ), Heat affected zone (HAZ), residual stress and strain distribution.

The objectives of this study is to develop two-dimension multi-pass FE model which predicts the transient temperature distributions, residual stress and strain distribution on 16mm thick multi-pass SM490 steel plate using Gas Metal Arc (GMA) welding process.

2 Development of FE Model

The welding process is a coupled thermo-mechanical phenomenon. Structural field are dependent on the thermal field whereas, structural field have very weak influence on the thermal fields. Thus this coupled welding phenomenon can be split into thermal analysis followed by structural analysis.

2.1 Thermal Analysis

The temporal temperature distribution $T(x,y,z,t)$ during welding process satisfies the following differential governing equation for three-dimensional heat conduction by the following equation;

$$\rho c_r \frac{\partial T}{\partial t}(x, y, z, t) = -\nabla \cdot q(x, y, z, t) + Q(x, y, z, t) \quad (1)$$

Where ρ is the density of the material (g/mm^3), c is the specific heat capacity ($\text{J/g}^\circ\text{C}$), T is the temperature ($^\circ\text{C}$), q is the heat flux vector (W/mm^2), Q is the internal heat generation rate (W/mm^3), x , y and z are the coordinates in the reference system (mm), t is the time (s) and ∇ is the spatial operator.

The non-linear isotropic Fourier's law is used to relate the heat flux vector to the thermal gradients;

$$q = -k\nabla T \quad (2)$$

where k is the temperature-dependent thermal conductivity.

The evolution thermal analysis is quite a complex phenomenon associated with GMA welding process. The weld pool shape can be largely influenced by the weld metal transfer mode and corresponding fluid flow dynamics. In representation of GMA welding, the most widely acceptable double heat source model presented by Goldaks is being used for the FE modeling [12]. The models give the Gaussian distribution for the butt weld and have excellent features of power and density distribution control in weld pool and HAZ. The Goldak's heat distributions are expressed by the following equations:

$$q(x, y, z) = \frac{\sqrt{3}cQ_w}{abc\pi\sqrt{\pi}} e^{-3x^2/a^2} e^{-3y^2/b^2} e^{-3z^2/c^2} \quad (3)$$

The parameter of moving heat source has been chosen to compute melted zone of thermal simulation are approximated as listed in Table1.

Table 1: Parameters used in double ellipsoidal heat source representation.

Weld type	Weld pass	a(mm)	b(mm)	c_f (mm)	c_r (mm)	f_f	f_r	η (%)	V(volt)	I(amp)	S(m/s)
Butt weld	1	5	5	6	14	0.6	1.4	90	35	330	0.22/60
	2	5.4	5.4	6	12.2	0.7	1.3		34	328	0.24/60
	3	4.39	11.89	6.87	25.4	0.5	1.5		32	300	0.27/60
	4	6	3.6	10.4	13.3	0.9	1.1		33	320	0.26/60
	5	8.8	2.5	7.4	14.8	0.7	1.3		33	318	0.26/60

In this simulation each pass process parameter is different to each other. The contribution of the transient temperature field is also dependent on temperature-dependent thermo-physical properties.

The combined heat transfer coefficient is expressed as follows;

$$h = 24.1 \times 10^{-4} \varepsilon T^{1.61} \quad (4)$$

where ϵ is emissivity of the surface of the body, a value of 0.9 is assumed for this study [12] and T is the temperature.

In this section, 2D thermal FE computational procedures has been developed to calculate the

temperature histories, residual stress and strain for multi-pass GMA welding process at 300 seconds of cooling time after every weld-pass. The dimension for five-pass finite element model is the 50mm in length and 16mm in thickness as shown in figure 1.

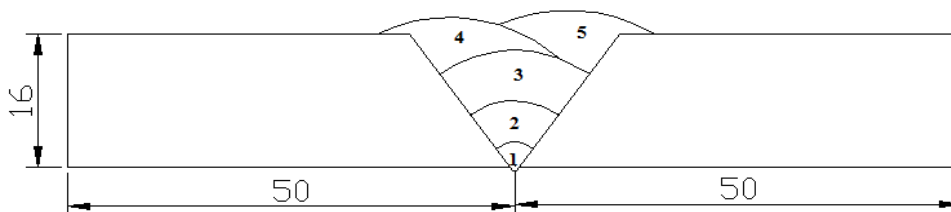


Figure 1: Dimension details and welds bead sequence for this study.

The welding conditions for all five-pass were chosen for this study as shown in Table 1. The diameter of the welding wire is used as 1.4mm. The efficiency η for the GMA welding process was assumed to be 0.9 [14]. The FE mesh density is fine in the vicinity of the weld centerline, while the meshes become gradually coarser away from welding zone in order to reduce the computer simulation time. The temperature dependent thermo-physical property for steel was assigned to the developed model shown in figure 2.

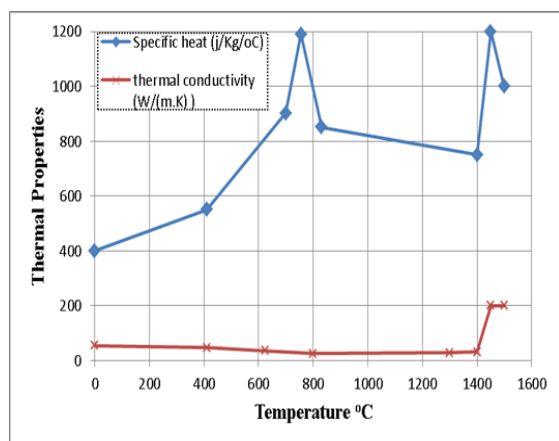


Figure 2: Thermo- physical properties of SM490 steel as a function of temperature.

2.2 Structural Simulation

For the mechanical analysis, the temperature history of each node from the preceding thermal analysis is input as the node load with temperature dependent mechanical properties. For SM490, phase transformation has a significant effect on residual

stress and deformation, therefore the thermo-elastic-plastic material model based on von Mises yield is formulated as follows;

$$\sigma_v = \sqrt{\frac{1}{2}[(\sigma_1 - \sigma_2)^2 + (\sigma_2 - \sigma_3)^2 + (\sigma_3 - \sigma_1)^2]} \quad (5)$$

The total strain can therefore be decomposed into three components as follows:

$$\epsilon^{total} = \epsilon^e + \epsilon^p + \epsilon^{th} \quad (6)$$

The component on the right-hand side of equation 6 corresponds to elastic, plastic and thermal strain, respectively.

The elastic strain is modeled using the isotropic Hooke's law with temperature-dependent Young's modulus and Poisson's ratio. For the plastic strain component, a plastic model is employed with the following features: the Von Mises yield surface and temperature-dependent material properties shown in figure 3.

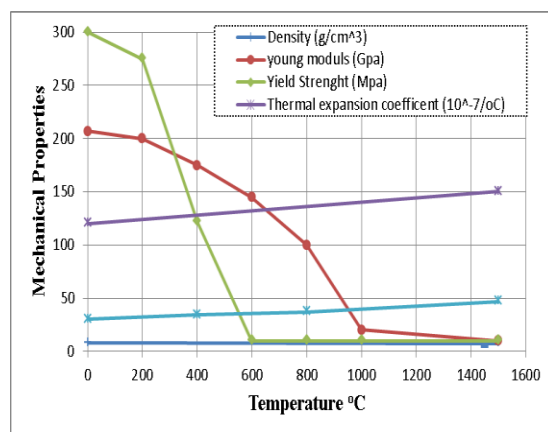


Figure 3: Thermo-mechanical properties of SM490 steel as a function of temperature.

3 Results and discussion

Figure 4 shows the temperature distributions during the GMA welding process, with the calculated weld penetration profile of FZ and HAZ after cooling of 300 seconds after each pass. The region temperature of HAZ and FZ is above 723°C and 1465°C respectively.

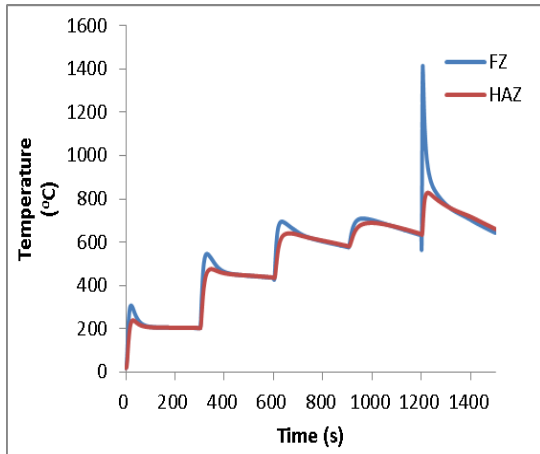
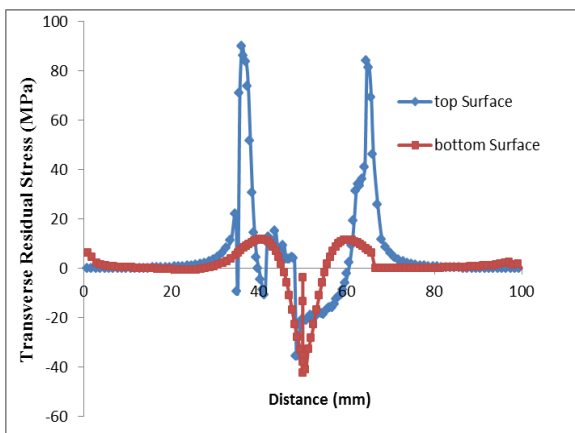


Figure 4: Fusion Zone and Heat Affect Zone with respect time on the plate.

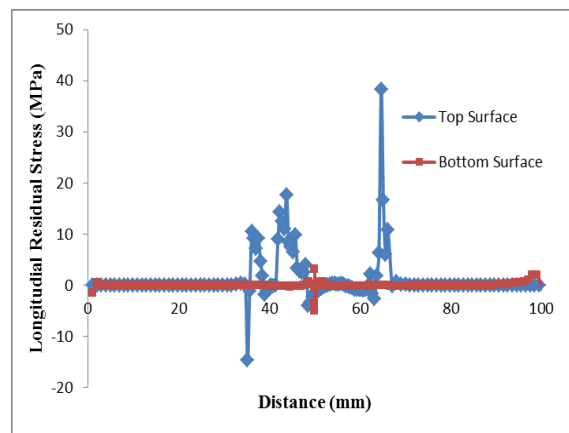
The numerical results of the mechanical analysis as shown in figure 5, exhibits the residual stress distribution transverses to the welding direction and as indicated in figure 6, the strain distribution is also in transverse direction along top and both surface of

the plate. The residual stresses on top and bottom surface of the plate are comparable for the both transverse and longitudinal direction. From figure 5(a), the both plates ends top surface has tensile stress and along HAZ tensile stress increase to about 90MPa, but at FZ and in vicinity of welding region is under compressive stress of about 40MPa. The stress at the top surface for left side plate fluctuates from tensile stress to compressive. This is due to fifth pass side which is more towards rights side and it has less heat load impact at left side of the plate. In comparison to the top surface, the bottom surface has tensile stress of about 10MPa and at the FZ and vicinity of welding region has large compressive stress of more than 42MPa.

Figure5 (b) shows the longitudinal residual stress at the top and bottom surface of the plate. The longitudinal residual stress along the top surface of both plates is uniform whereas low tensile and compressive stress is until FZ. In FZ the stress fluctuate from compressive and tensile stress at the left side of the plate. At the right side plate, initially longitudinal stress at FZ is tensile stress and as approaches the fifth pass region the stress is compressive. The longitudinal stress at the bottom surface is low and uniform until the welding region, where stress increase a little to tensile than to compression. In comparison of transverse and longitudinal stress distribution, there is large range and magnitude stress observed in transverse stress distribution.



(a) Transverse residual stress



(b) Longitudinal residual stress

Figure 5: Numerically calculated transverse and longitudinal residual stress of 5beads GMA welding process.

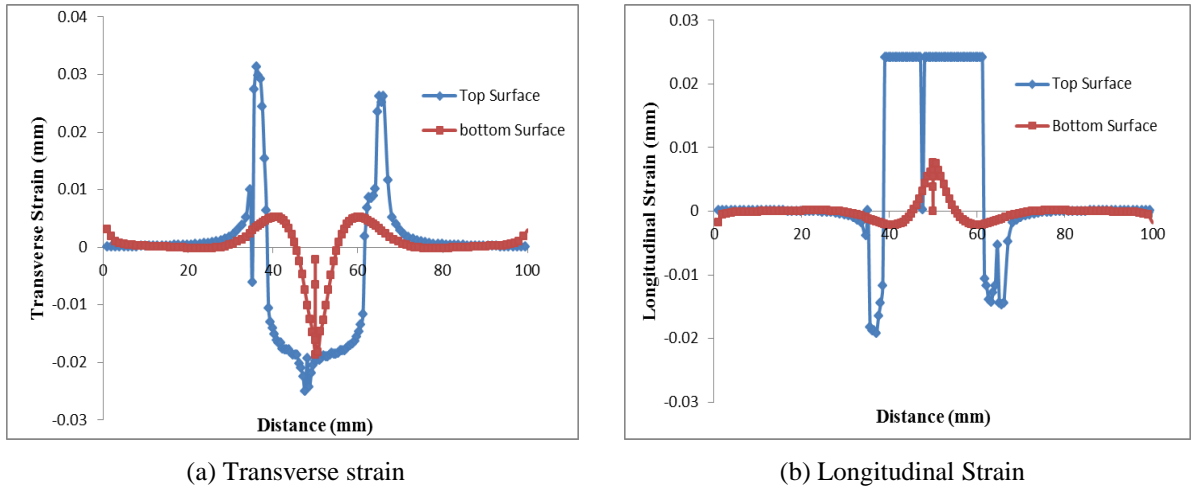


Figure 6: Numerically calculated transverse and longitudinal strain of 5 beads GMA welding.

This is due to both plates restrained in transverse direction during the welding process. Figure 6(a) shows the transverse elastic strain distribution at the top and bottom surface of the plate. It can be observed that the elastic strain distribution predicted for the top and bottom surface has a significant difference. The large tensile strain at the top surface is mostly concentrated around FZ and HAZ compared to the bottom surface of the plate, but at the welding region the large compressive strain is observed for both the plate surfaces.

The large strain at the top surface is due to heat load applied to the fourth and fifth weld-pass. For longitudinal strain, it is observed that both the top and bottom surface of the plate, have compressive strain at HAZ and FZ whereas in vicinity of welding region it has tensile strain. In comparison the range and magnitude distribution of transverse and longitudinal strain, the transverse strain range is larger than that of the longitudinal strain distribution.

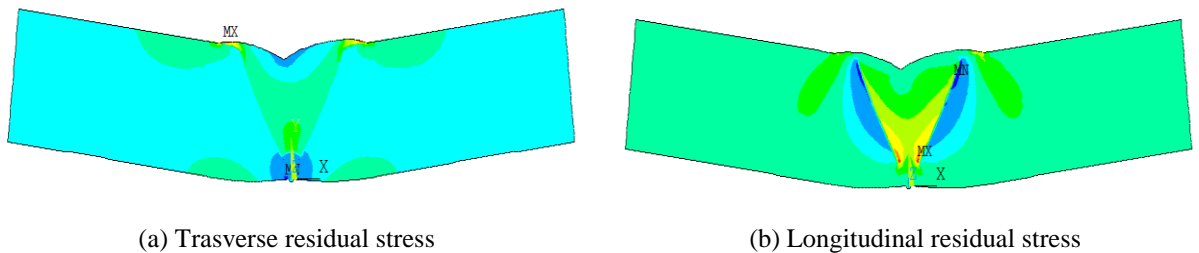


Figure 7: Transverse and Longitudinal residual stress distribution profile of 5beads GMA welding process.

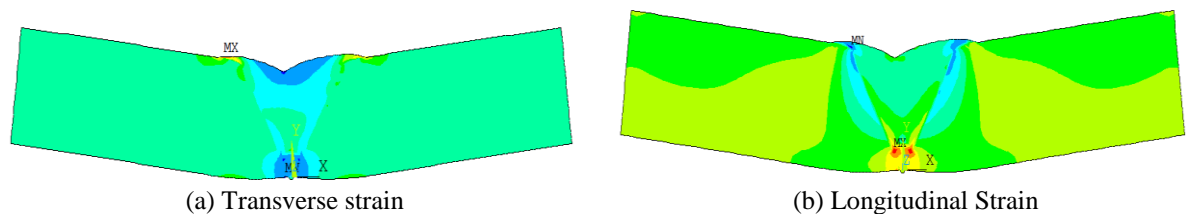


Figure 8: Transverse and Longitudinal strain distribution profile of 5beads GMA welding process.

Figure 7 and 8 shows residual stress and strain distribution profile of 5 pass welding process. The profile history indicates HAZ and FZ are under large stress. Generally, the range and magnitude of strain are mainly governed by the peak temperatures and the restraint conditions. The restraint intensity in this case is in the transverse direction, therefore this result in magnitude of transverse strain large.

4 Conclusions

This present study investigation shows that the two dimension numerical analysis could be used to predict the temperature field, residual stress and strain distribution in thick five pass butt-weld joint.

Based on the simulation results, it is know that residual stress and strain distribution on top and bottom surface of the plate differs, due to heat distribution load applied to plate, the heat input and also the cooling time after each welding pass. The restraint of plate has also impact on residual stress and strain. This is shown the figures 5 and 6. The plates were restraint in the transverse direction of welding, before large stress and strain is noted in transverse direction.

The elastic FEM can be used to predict precisely the welding deformation, residual stress and strain in a thick multi pass butt welding. Furthermore, the extensive experiment effort of component testing could reduce adequate and deliberate application of welding simulation.

Acknowledgements

This research was financially supported by the Ministry of Education, Science Technology (MEST) and National Research Foundation of Korea (NRF) through the Human Resource Training Project for Regional Innovation.

References

- [1] Heinze C., Schwenk C., Rethmeier M., 2012. Numerical calculation of residual stress development of multi-pass gas metal arc welding under a high restraint conditions, *Material and Design*, 35: 201-209
- [2] Attaeha M.J. and Sattari-Far I., 2011. Study on welding temperature distribution in thin weld plate through experimental measurement and finite element simulation, *Journal of Materials Processing Technology*. 211: 688-694
- [3] Doan T.T., Vo T.Q and Kim I.S., 2010. *Finite Element Predictions of Residual Stress and Distortion*, 11th Asia Pacific Industrial Engineering and Management System, October 7-10; Melaka, Malaysia
- [4] Deng D. and Murakawa H., 2008. Prediction of Welding Distortion and Residual Stress in a thin plate Butt-Weld Joint, *Computational Materials Science* 43(3): 353-365.
- [5] Liang G., Yuan S., 2008. Study on the temperature measurement of AZ31B magnesium alloy in gas tungsten arc welding, *Mater. Lett.* 62, 2282–2284,
- [6] Duranton P., Devaux J., Robin V., Gilles P. and Bergheau J.M., 2004. 3D Modeling of Multipass Welding of a 316L Stainless Steel Pipe, *Journal of Materials Processing Technology*, p.153-154, 457-463,
- [7] Zhu X.K., Chao Y.J., 2002, Effects of temperature-dependent material properties on welding simulation, *Computers and Structural*. 80, p.967–976
- [8] Lee H.T. and Wu J.L., 2009. The effects of peak temperature and cooling rate on the susceptibility to intergranular corrosion of alloy 690 by laser beam and gas tungsten arc welding, *Corrosion Science* 51: 439-445
- [9] Goldak J. A. and Akhlaghi M., 2005, *Computational welding Mechanics*, Springer
- [10] Lu F., Yao S., Lou,S. and Li Y., (2004). Modeling and finite element analysis on GTAW arc and weld pool, *Computational Materials Science* 29(3), p. 371–378
- [11] Lee C.H. and Chang K.H., 2008. Three dimensional finite element simulation of residual stresses in circumferential welds of steel pipe including pipe diameter effects, *Materials Science & Engineering A* 487(1-2): 210–218,
- [12] Goldak J., Chakravarti A. and Bibby M., 1984, A new finite element model for welding heat sources, *Metallurgical and Materials Transactions B* 15(2), p. 299–305,
- [13] Nguyen N.T., Ohta A., Matsuoka K., Suzuki N. and Maeda Y., 1999, Analytical solutions for transient temperature of semi-infinite body subjected to 3-D moving heat sources, *Welding Journal Research Supplement*, August, p.265-274

- [14] Doan T.T., 2009 Experimental and Numerical Study for the Automatic GMA Welding Process, Thesis (PhD), Mokpo National University